Supporting Information

Chou et al. 10.1073/pnas.1424684112

SI Methods

Reagents Used. For synthesis of small molecule conjugates, the following reagents were purchased from Sigma-Aldrich: 12-aminododecanoic acid, [1,1′-Bis(diphenylphosphino)ferrocene] dichloropalladium(II) complexed with dichloromethane [Pd(dppf)Cl_2·DCM], lithium hydroxide, triethylamine, bis(pinacolato)diboron, potassium acetate, 4-carboxyphenylboronic acid, 4-bromosulfonyl chloride, 3-carboxy-5-nitrophenylboronic acid, dichloromethane, ethyl acetate, methanol, and dioxane. 4-Carboxy-3-fluorophenylboronic acid was purchased from Optima Chemical. *O*-(benzotriazol-1-yl)-*N,N,N′,N′*-tetramethyluronium tetrafluoroborate (TBTU) was purchased from AnaSpec.

For insulin modification, myristic acid, *N,N′*-dicyclohexylcarbodiimide, and *N*-hydroxysuccinimide were purchased from Sigma Aldrich. Animal origin free recombinant human insulin was purchased from Life Technologies.

Synthesis of Small Molecule Conjugates. Please refer to Scheme S1 for a detailed synthetic strategy.

12-(4-Boronobenzamido)dodecanoic acid (1). (4-((12-Methoxy-12-oxododecyl)carbamoyl)phenyl)boronic acid **8** (4.22 g, 11.20 mmol) and lithium hydroxide (1.35 g, 55.97 mmol) were dissolved in a 3:1 MeOH/water solution (80 mL). The reaction was stirred overnight under nitrogen, and the solvent was removed in vacuo. The reaction was then dissolved in water and acidified to pH 1 using 1 N HCl, and the precipitate was collected by filtration. Column chromatography (0–20% MeOH in DCM) gave a white product (2.64 g, 7.28 mmol, 65%).

^{1}H NMR (CD_3OD) δ7.73 (d, 2H), δ7.67 (d, 2H), δ3.27 (t, 2H), δ2.22 (t, 2H), δ1.56 (m, 4H), δ1.30 (m, 14H)

^{13}C NMR (CD_3OD) δ177.0, 133.9, 126.5, 100.5, 40.4, 34.2, 29.9, 29.7, 29.5, 27.4, 25.4

High-resolution mass spectrometry (HRMS): calculated 363.2217; found: 363.2291

12-(4-Borono-2-fluorobenzamido)dodecanoic acid (2). (3-Fluoro-4-((12-methoxy-12-oxododecyl)carbamoyl)phenyl)boronic acid **9** (5.15 g, 13.04 mmol) and lithium hydroxide (1.56 g, 65.20 mmol) were dissolved in a 3:1 MeOH/water solution (80 mL). The reaction was stirred overnight under nitrogen, and the solvent was removed in vacuo. The reaction was then dissolved in water and acidified to pH 1 using 1 N HCl, and the precipitate was collected by filtration. Column chromatography (0–20% MeOH in DCM) gave a white product (3.23 g, 8.48 mmol, 65%).

^{1}H NMR (CD_3OD) δ7.73 (m, 3H), δ3.35 (t, 2H), δ2.26 (t, 2H), δ1.60 (m, 4H), δ1.31 (m, 14H)

^{13}C NMR (CD_3OD) δ177.0, 129.7, 127.7, 121.1, 121.0, 40.3, 34.2, 29.9, 29.7, 29.5, 27.3, 25.4

HRMS: calculated 381.2123; found: 381.2124

12-(3-Borono-5-nitrobenzamido)dodecanoic acid (3). (3-((12-Methoxy-12-oxododecyl)carbamoyl)-5-nitrophenyl)boronic acid **10** (1.02 g, 2.43 mmol) and lithium hydroxide (0.29 g, 12.13 mmol) were dissolved in a 3:1 MeOH/water solution (40 mL). The reaction was stirred overnight under nitrogen, and the solvent was removed in vacuo. The reaction was then dissolved in water and acidified to pH 1 using 1 N HCl, and the precipitate was collected by filtration. Column chromatography (0–20% MeOH in DCM) gave a white product (0.64 g, 1.88 mmol, 65%).

^{1}H NMR (CD_3OD) δ8.58 (m, 2H), δ8.45 (s, 1H), δ3.34 (t, 2H), δ2.20 (t, 2H), δ1.54 (m, 4H), δ1.22 (m, 14H)

^{13}C NMR (CD_3OD) δ177.1, 167.2, 148.5, 138.7, 136.0, 131.0, 123.9, 40.6, 30.0, 29.8, 29.6, 27.4, 25.4

HRMS: calculated 408.2068; found: 408.2068

12-((4-Boronophenyl)sulfonamido)dodecanoic acid (4). Methyl 12-((4-(4,4,5,5-tetramethyl-1,3,2-dioxaborolan-2-yl)phenyl)sulfonamido) dodecanoate **11** (2.71 g, 5.47 mmol) and lithium hydroxide (1.56 g, 65.20 mmol) were dissolved in a 3:1 MeOH/water solution (80 mL). The reaction was stirred overnight under nitrogen, and the solvent was removed in vacuo. The reaction was then dissolved in water and acidified to pH 1 using 1 N HCl, and the precipitate collected by filtration. Column chromatography (0–20% MeOH in DCM) gave a white product (1.4 g, 3.56 mmol, 65%).

^{1}H NMR (CD_3OD): δ7.84 (d, 2H), δ7.82 (d, 2H), δ3.31 (t, 2H), δ2.84 (t, 2H), δ2.27 (m, 2H), δ1.59 (m, 2H), δ1.26 (14H)

^{13}C NMR (CD_3OD): δ177.0, 134.5, 126.1, 116.7, 43.3, 34.2, 29.8, 29.7, 29.5, 26.9, 25.4

HRMS: calculated 399.1887; found: 399.1900

Methyl 12-((4-bromophenyl)sulfonamido)dodecanoate (7). Methyl 12-aminododecanoate **6** (5.08 g, 22.19 mmol) and 4-bromosulfonyl chloride (4.73 g, 18.49 mmol) were dissolved in dichloromethane (100 mL) with triethylamine (7.73 mL, 55.47 mmol). The reaction was stirred overnight, and the solvent was removed in vacuo. The reaction was then dissolved in ethyl acetate and extracted with water and brine. The organic layer was dried with $MgSO_4$ and evaporated in vacuo. Column chromatography (0–20% MeOH in DCM) gave a white product (6.2 g, 13.84 mmol, 75%).

^{1}H NMR (CD_3OD) δ7.73 (d, 2H), δ7.67 (d, 2H), δ3.67 (s, 3H), δ2.96 (t, 2H), δ2.31 (t, 2H), δ1.59 (m, 2H), δ1.48 (m, 2H), δ1.22 (m, 14H)

^{13}C NMR (CD_3OD) δ175.1, 139.8, 133.0, 129.3, 128.0, 52.1, 43.9, 34.8, 30.1, 29.9, 29.8, 29.7, 27.1, 25.6

HRMS: calculated 447.1079; found: 447.1094

(4-((12-Methoxy-12-oxododecyl)carbamoyl)phenyl)boronic acid (8). Methyl 12-aminododecanoate **6** (2.00 g, 8.73 mmol), 4-carboxyphenylboronic acid (2.18 g, 13.10 mmol), and TBTU (4.21 g, 13.10 mmol), were dissolved in a 1:1 dimethylformamide (DMF)/pyridine solution (100 mL). The reaction was stirred overnight under nitrogen, and the solvent was removed in vacuo. The reaction was dissolved in ethyl acetate and extracted with 30% citric acid and brine. The organic layer was dried with $MgSO_4$ and evaporated in vacuo. Column chromatography (0–20% MeOH in DCM) gave a white product (2.84 g, 7.53 mmol, 85%).

^{1}H NMR (CD_3OD) δ7.77 (d, 2H), δ7.71 (d, 2H), δ3.62 (s, 3H), δ3.27 (t, 2H), δ2.27 (t, 2H), δ1.55 (m, 4H), δ1.25 (m, 14H)

^{13}C NMR (CD_3OD) δ175.3, 168.2, 134.1, 128.7, 126.5, 110.7, 51.3, 40.4, 38.2, 36.3, 34.1, 31.2, 29.7, 27.4, 20.1

HRMS: calculated 377.2374; found: 377.2378

(3-Fluoro-4-((12-methoxy-12-oxododecyl)carbamoyl)phenyl)boronic acid (9). Methyl 12-aminododecanoate **6** (2.00 g, 8.73 mmol), 4-carboxy-3-fluorophenylboronic acid (2.41 g, 13.10 mmol), and TBTU (4.21 g, 13.10 mmol) were dissolved in a 1:1 DMF/pyridine solution (100 mL). The reaction was stirred overnight under nitrogen, and the solvent was removed in vacuo. The reaction was dissolved in ethyl acetate and extracted with 30% citric acid and brine. The organic layer was dried with $MgSO_4$ and evaporated in vacuo. Column chromatography (0–20% MeOH in DCM) gave a white product (2.98 g, 7.53 mmol, 85%).

^{1}H NMR (CD_3OD) δ7.65 (m, 3H), δ3.64 (s, 3H), δ3.35 (t, 2H), δ2.30 (t, 2H), δ1.59 (m, 4H), δ1.30 (m, 14H)

^{13}C NMR (CD_3OD) δ175.3, 166.1, 161.1, 159.1, 129.8, 121.2, 121.1, 51.3, 40.3, 34.1, 30.0, 29.7, 29.5, 27.3, 25.3

HRMS: calculated 395.2279; found: 395.2293

(3-((12-Methoxy-12-oxododecyl)carbamoyl)-5-nitrophenyl)boronic acid (10). Methyl 12-aminododecanoate 6 (2.00 g, 8.73 mmol), 3-carboxy-5-nitrophenylboronic acid (2.78 g, 13.10 mmol), and TBTU (4.21 g,

13.10 mmol) were dissolved in a 1:1 DMF/pyridine solution (100 mL). The reaction was stirred overnight under nitrogen, and the solvent was removed in vacuo. The reaction was dissolved in ethyl acetate and extracted with 30% citric acid and brine. The organic layer was dried with $MgSO_4$ and evaporated in vacuo. Column chromatography (0–20% MeOH in DCM) gave a pale yellow product (3.18 g, 7.53 mmol, 85%).

^{1}H NMR (CD_3OD) δ8.60 (m, 2H), δ8.45 (s, 1H), δ3.59 (s, 3H), δ3.35 (t, 2H), δ2.23 (t, 2H), δ1.55 (m, 4H), δ1.23 (m, 14H)

^{13}C NMR (CD_3OD) δ175.3, 167.1, 148.5, 138.6, 136.0, 130.9, 123.7, 51.3, 40.6, 34.1, 29.9, 29.7, 29.5, 27.4, 25.3

HRMS: calculated 422.2224; found: 422.2223

Methyl12-((4-(4,4,5,5-tetramethyl-1,3,2-dioxaborolan-2-yl)phenyl)sulfonamido) dodecanoate (11). Methyl 12-((4-bromophenyl)sulfonamido) dodecanoate **7** (2.96 g, 6.61 mmol), bis(pinacolato)diboron (2.52 g, 9.91 mmol), Pd(dppf)Cl_2·DCM (0.81 g, 0.9 mmol), and potassium acetate (2.60 g, 26.43 mmol) were dissolved in dioxane (100 mL) and refluxed under nitrogen overnight. The reaction was filtered through Celite, and the solvent was removed in vacuo. The reaction was dissolved in ethyl acetate and extracted with water and brine. The organic layer was dried with $MgSO_4$ and evaporated in vacuo. Column chromatography (0–20% MeOH in DCM) gave a white product (2.71 g, 5.47 mmol, 85%).

^{1}H NMR (CD_3OD) δ7.90 (d, 2H), δ7.84 (d, 2H), δ3.65 (s, 3H), δ2.84 (t, 2H), δ2.31 (t, 2H), δ1.58 (m, 2H), δ1.43 (m, 2H), δ1.36 (12H), δ1.22 (m, 14H)

^{13}C NMR (CD_3OD) δ175.3, 143.8, 135.5, 126.4, 85.0, 51.3, 43.3, 34.1, 29.9, 29.8, 29.7, 29.5, 26.9, 25.3, 24.5

HRMS: calculated 495.2826; found: 495.2853

Insulin Modification. The small molecule, **1**, **2**, **3**, **4**, or myristic acid (20.67 μmol), *N,N′*-dicyclohexylcarbodiimide (4.26 mg, 20.67 μmol), and *N*-hydroxysuccinimide (2.38 mg, 20.67 μmol) were dissolved in tetrahydrofuran (1 mL) and stirred for 4 h at room temperature. Recombinant human insulin (100 mg, 17.23 μmol) was dissolved in 0.1 M Na_2CO_3 (1 mL) and then added to stirring small molecule reaction. After 1 h, 0.2 M CH_3NH_2 (1 mL) and 6 N HCl (26 μL) were added to the reaction mixture. The resulting solution and precipitate were centrifuged, and the pellet was resuspended in DMSO (2 mL). The product was purified via reversed phase preparative HPLC using an Atlantis C_{18} column (250 × 10 mm, 5 μm; Waters), with a mobile phase gradient from 95% to 5% (vol/vol) of acetic acid (1.5%) in H_2O in acetonitrile. Fractions were collected and lyophilized to provide a white product. The product was characterized by deconvolution ESI using a QSTAR hybrid Q-TOF, through the Koch Institute Swanson Biotechnology Center Biopolymers and Proteomics core. Masses obtained were as follows: Ins-PBA-A, expected: 6189, actual 6153; Ins-PBA-F, expected: 6153, actual 6115; Ins-PBA-N, expected: 6171, actual 6135; Ins-PBA-S, expected: 6198, actual 6162; Ins-LA-C14, expected 6018, actual 6018. It is noted that these masses are consistent with MS for PBA-modified peptides, where the double-dehydrated mass (i.e., −36) is observed due to gas phase anhydro formation of the boronic acid (1).

To confirm the B29 modification, the modified insulin was reduced through DTT, free thiols were alkylated, and then the protein was digested with trypsin. Proteomics analysis was performed using a QSTAR hybrid Q-TOF, with tandem MS/MS analysis and Mascot analysis at the Koch Institute Swanson Biotechnology Center Biopolymers and Proteomics core. The search was conducted with masses for the digested products with free amines at the A1, B1, and Lys_{B29} positions, as well as the small molecule-conjugated mass (di-anyhdro mass for PBA-containing conjugates).

Circular Dichroism. Near infrared circular dichroism was performed at an insulin concentration in water of 0.25 mg/mL using a 1-mm path length quartz cuvette. Spectra were collected using a Jasco J-1500 high performance circular dichroism spectrometer over a wavelength range of 190–240 nm.

Insulin Receptor Activation. CHO-M1 cells (ATCC) were seeded at 25,000 cells per well in a 96-well plate and allowed to grow for 24 h before serum starving overnight. Serum-starved cells were treated with insulin derivatives at 10 μg/mL for 30 min. Following stimulation, cells were lysed, and phosphorylated AKT at Ser473 was assayed using a commercially available kit (HTRF; Cisbio) in accordance with the manufacturer's protocol.

Determination of Binding Kinetics. To determine the binding kinetics of Ins-PBA-F, Ins-LA-C14, and native insulin to human serum albumin, biolayer interferometry was used (Octet RED; ForteBio). Amine-Reactive Second Generation Dip and Read Biosensors (AR2G) were used in this study. Tips were activated for 300 s in a solution of 20 mM *N*-(3-dimethylminopropyl)-*N* ethylcarbodiimide hydrochloride (EDC; Sigma) and 10 mM *N*-hyrdoxysulfosuccinimide sodium salt (sulfo-NHS; Sigma) in H_2O. Following this, tips were transferred to a solution of fatty acid-free human serum albumin (HSA; Sigma) at 5 μg/mL in pH 5.0 sodium acetate buffer for 800 s. Tips were subsequently quenched for 500 s in a 1 M ethanolamine solution at pH 8.5 (ForteBio). The association of insulin or insulin derivatives was monitored at concentrations of 50, 75, 100, and 125 μg/mL, with association performed for 300 s. Insulin was dissolved in either PBS or PBS plus 5 mg/mL glucose, and a baseline for each tip was performed in this buffer before association. Dissociation was monitored for 600 s in PBS or PBS with 5 mg/mL glucose. Baseline-adjusted sensograms were fit to a 1:1 binding model using ForteBio analysis software.

Diabetic Mouse Model. Male C57BL/6J mice, age 8 wk, were purchased Jackson Laboratory. After acclimation, mice were fasted for 4 h before i.p. injection of 150 mg/kg STZ (Sigma). STZ for injection was dissolved at a concentration of 22.5 mg/mL in 2.94% (wt/vol) in pH 4.5 sodium citrate buffer immediately before injection. Mice were allowed to eat ad libitum, and glucose levels were monitored by peripheral tail vein bleeds using a portable glucose meter (Accu-Chek Aviva; Roche) daily until unfasted glucose levels were >400 mg/dL. For healthy mouse studies, age-matched healthy C57BL/6J mice were used.

Glucose Tolerance Test. STZ-induced diabetic mice were fasted overnight before performing studies. Mice were bled at the beginning of the study, and any mouse with a fasting blood glucose level <300 mg/dL was triaged from the study. Mice were then randomized and injected s.c. with native insulin or insulin variants at doses ranging from 34.7 to 173.5 μg/kg. Blood glucose readings were collected every 15–30 min using a handheld glucose meter. A glucose tolerance test was performed via i.p. injection of 1 g/kg glucose dissolved in water, and blood glucose was monitored. Responsiveness was quantified by measuring the area under the curve with a baseline at the point of glucose injection and integrating across a 3-h window following challenge. For dosing studies in healthy mice, insulin injections were performed via identical methods, but no glucose tolerance test was performed. The induction of hypoglycemia was quantified as the difference between initial and nadir (i.e., lowest observed) blood glucose readings divided by the time at which nadir was reached to determine the hypoglycemia index. For fructose challenge, studies were performed identically, with exception of i.p. injection of 1 g/kg fructose to perform the challenge.

Continuous Glucose Monitoring. Continuous glucose monitoring was performed using human continuous glucose monitors (Medtronic iPro2). CGM sensors were implanted s.c. in mice

following adaptation of manufacturer's instructions. For implantation, mice were briefly anesthetized by inhaled isoflurane, and fur around the abdomen and back was removed using electric clippers. The skin was then cleaned with an alcohol prep wipe, and the s.c. sensor was inserted under the skin with the supplied guide needle. The guide needle was subsequently removed, and the recording device was attached to the sensor. Anchoring to the skin was achieved with the attached adhesive patch in addition to surgical tape. The device was calibrated with two readings on a handheld glucose meter over the following 2 h. After calibration, mice were injected with insulin derivatives as above, and glucose tolerance tests were performed as described.

1. Hoeg-Jensen T, et al. (2005) Insulins with built-in glucose sensors for glucose responsive insulin release. *J Peptide Sci* 11(6):339–346.

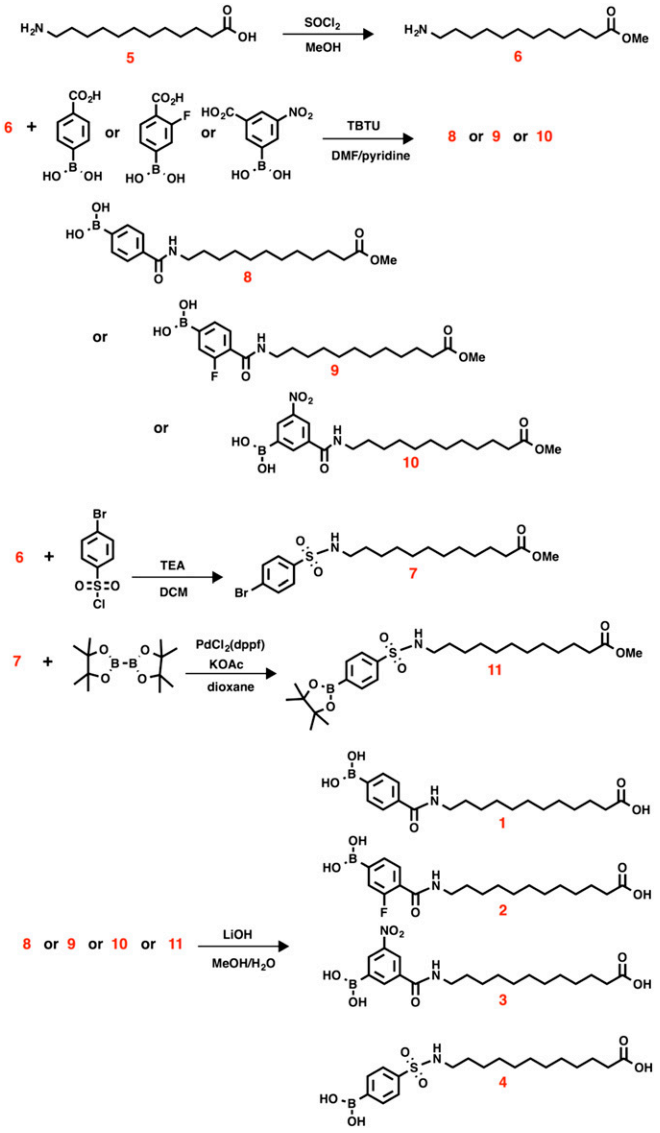

Scheme S1. Synthetic route for preparation of small molecule conjugates.

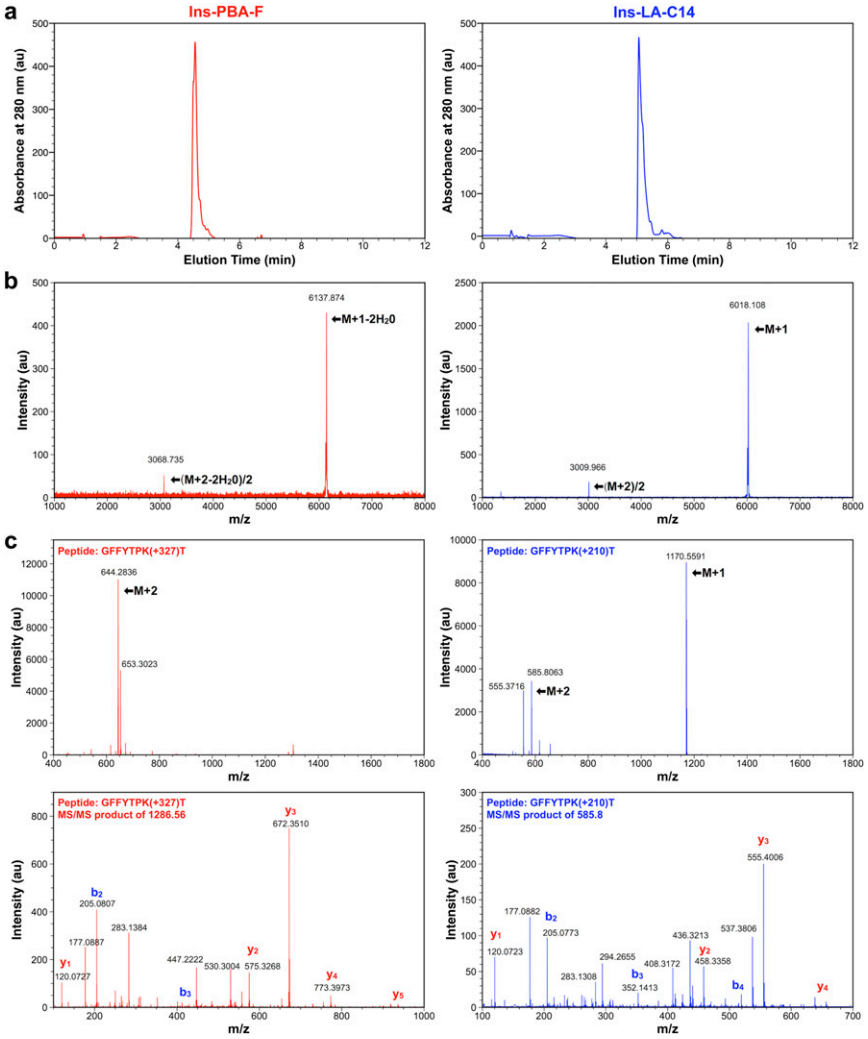

Fig. S1. Validation of insulin modification and purification for Ins-PBA-F (*Left*) and Ins-LA-C14 (*Right*). Shown are results from (*A*) analytical reversed-phase HPLC of the purified product, (*B*) MALDI-TOF MS of the purified product, and (*C*) DTT/trypsin digestion and ESI-MS/MS proteomic analysis of both insulin derivatives identifying the modification specifically on the B29 fragment and MS/MS sequence identification for this fragment.

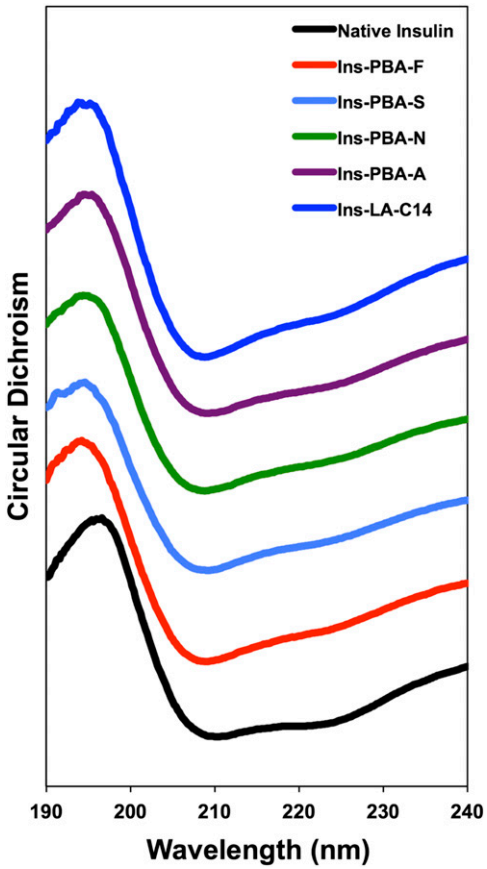

Fig. S2. Near-UV circular dichroism spectroscopy of all modified insulins developed in this study. Spectra have been shifted along the *y* axis for ease in presentation and comparison of circular dichroism signatures.

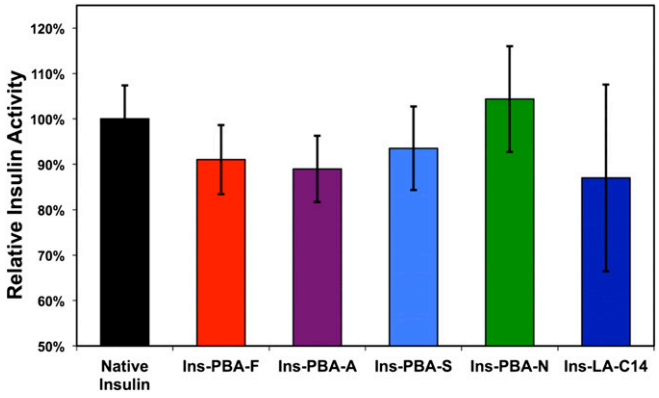

Fig. S3. Insulin activity measured by phosphorylation of the insulin receptor in vitro. Receptor activation is expressed relative to native insulin. No significant differences between insulin derivatives were observed.

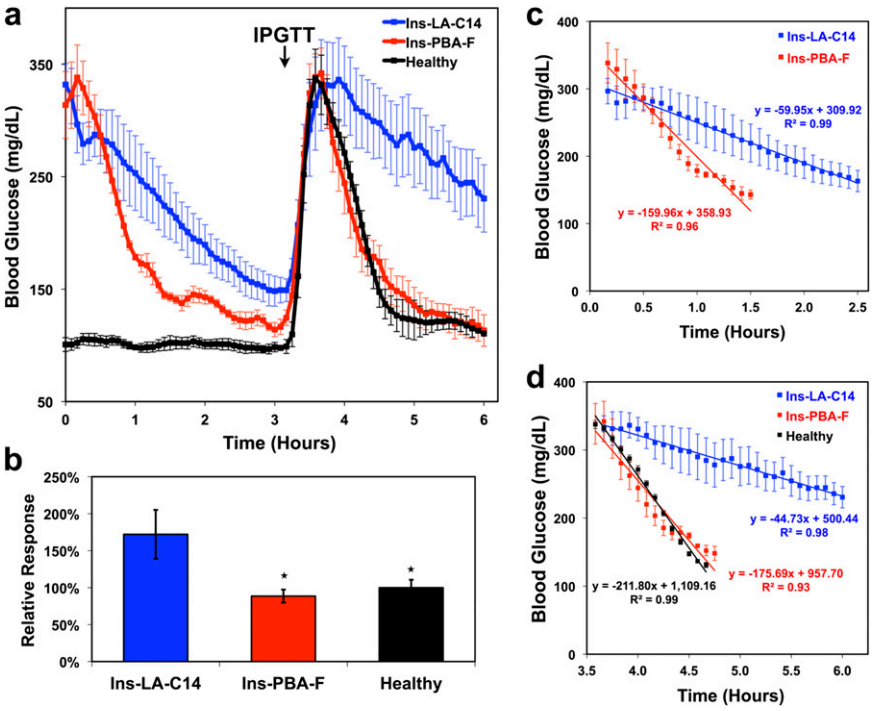

Fig. S4. Assessment of response kinetics using continuous glucose monitoring. (*A*) Blood glucose levels following treatment at time 0 with a dose of 3 IU/kg (104.1 μg/kg) of either Ins-PBA-F or Ins-LA-C14 in STZ-induced diabetic mice in comparison with healthy mice that were not injected with insulin. At 3 h following insulin administration, an IPGTT was performed in all three groups. (*B*) The responsiveness of each insulin in comparison with a healthy functional pancreas control was calculated based on the area under the curve from 3 to 6 h, with the baseline set at the 3-h blood glucose reading. (*C*) Analysis of the response rate following insulin administration in a hyperglycemic state until a normoglycemic state is reached for Ins-PBA-F and Ins-LA-C14. (*D*) Analysis of the response rate from the peak following glucose challenge for Ins-PBA-F, Ins-LA-C14, and the healthy control. $^{\star}P < 0.05$ for Ins-PBA-F and healthy controls compared with Ins-LA-C14.

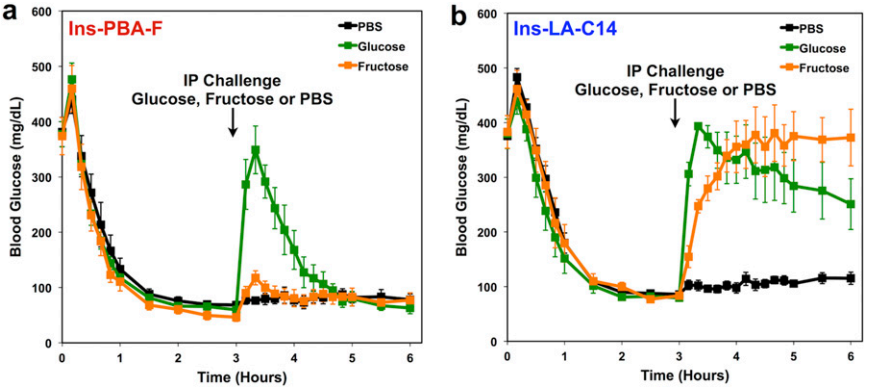

Fig. S5. Assessment of insulin activation by a nonglucose diol (fructose) with monitoring of blood glucose levels in and STZ-induced diabetic mouse model. Injections of (*A*) Ins-PBA-F or (*B*) Ins-LA-C14 were administered at time 0 at a dose of 3 IU/kg (104.1 μg/kg). At 3 h, animals were challenged by an i.p. injection of glucose (1 g/kg), fructose (1 g/kg), or PBS.

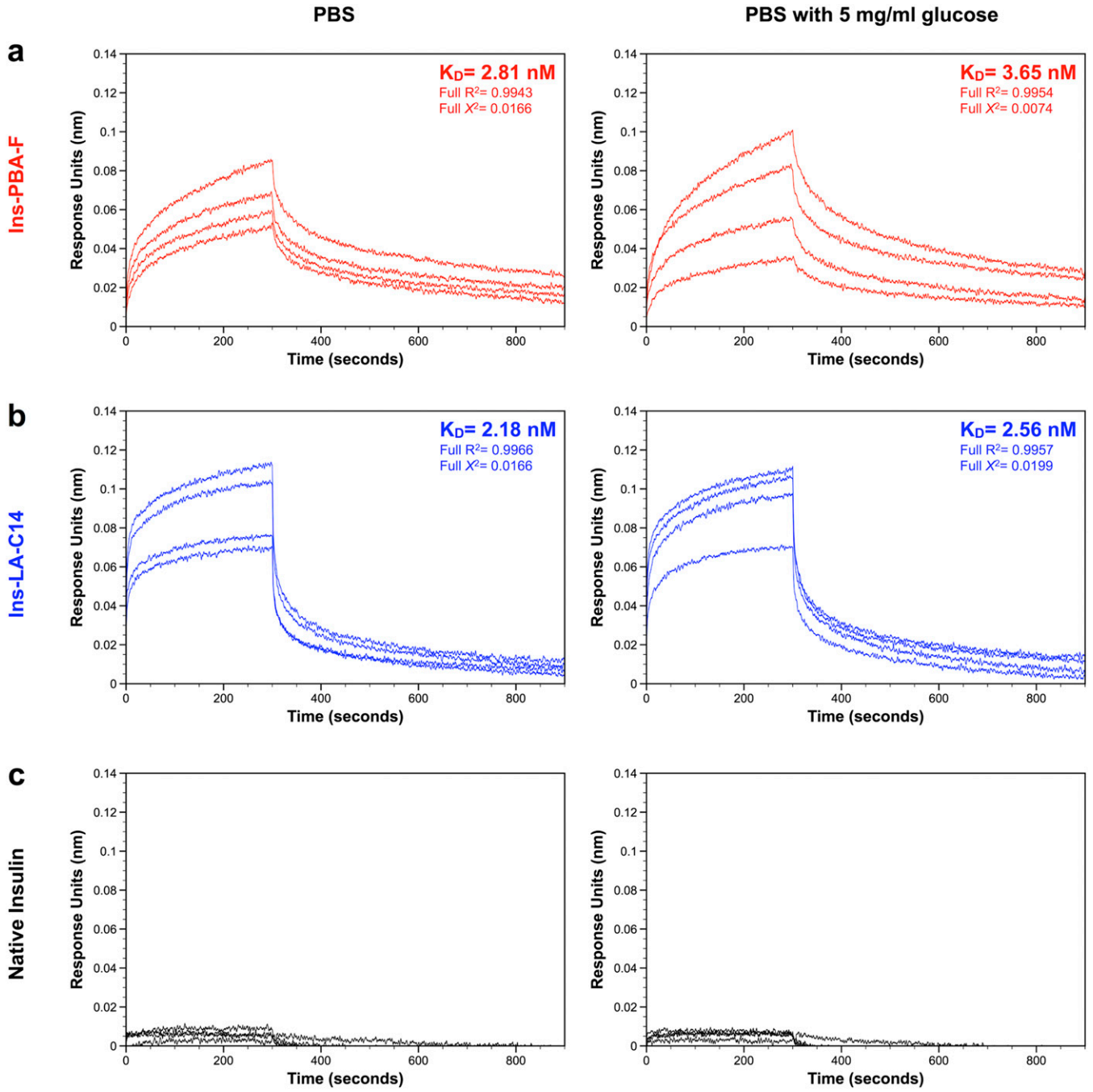

Fig. S6. Response curves from biolayer interferometry measurements for binding affinity to human serum albumin of (*A*) Ins-PBA-F, (*B*) Ins-LA-C14, or (*C*) native insulin. The association phase was carried out for 300 s, followed by dissociation for 600 s. Both association and dissociation were carried out in either PBS (*Left*) or PBS supplemented with 5 mg/mL (500 mg/dL) glucose (*Right*). Four concentrations of each insulin were evaluated in the association phase (50, 75, 100, or 125 μg/mL), and full response curves were fit to a 1:1 binding model using the ForteBio Octet RED analysis software. Results for the observed binding constant along with R^2 and χ^2 values for the fits are shown for Ins-PBA-F and Ins-LA-C14. Data for native insulin could not be fit to binding models. Based on a series of analyses, there were no differences in binding constants for each insulin derivative in the presence or absence of glucose.